

# Electronic Supplementary Information

Impact of metal exchange on the electronic structure and optical properties of isostructural octa-coordinated  $\text{Mo}^{\text{IV}}/\text{Cd}^{\text{II}}$  and  $\text{W}^{\text{IV}}/\text{Cd}^{\text{II}}$  polynuclear cyanide polymers

R. Mojica,<sup>1,a</sup> Y. Ávila,<sup>a</sup> P. Morgado,<sup>a</sup> M. C. Vázquez,<sup>a</sup> J. Rodríguez-Hernández,<sup>b</sup> P. M. Crespo,<sup>c</sup>  
and E. Reguera<sup>2,a</sup>

<sup>a</sup> *Centro de Investigación en Ciencia Aplicada y Tecnología Avanzada, Unidad Legaríá, Instituto Politécnico Nacional, 11500, Miguel Hidalgo, Ciudad de México, México.*

<sup>b</sup> *Centro de Investigación en Química Aplicada, 25294, Saltillo, Coahuila, México.*

<sup>b</sup> *Universidad Tecnológica de Izúcar de Matamoros, 74420, Izúcar de Matamoros, Puebla, México.*

---

---

<sup>1</sup> Corresponding Author. Email: rodrigo1993mx@gmail.com (R. Mojica) Tel: (+52) 55 5729 6000 Op. 67797

<sup>2</sup> Corresponding Author. Email: ereguerar@ipn.mx (E. Reguera) Tel: (+52) 55 5729 6000 Op. 67797

# 1 Bader charge analysis

Table S 1: Bader charge analysis. The showed values correspond with the HSE06 density functional computations. For the M and Cd metals the average value of the total of Bader charges is shown. For the cyano ligands cases (CN) the total average ( $CN_{avg}$ ) is showed together with the charge values of four different types of CN ligands differentiated by their positions in the dodecahedron, as it is depicted in Figure 1 of ESI.

Bader charge analysis, [ $bohr^{-3}$ ]							
System	M	Cd	$CN_{avg}$	$CN_{T1}$	$CN_{T2}$	$CN_{T3}$	$CN_{T4}$
<b>Cd-Mo</b> ( $Cd_2(H_2O)_4[Mo(CN)_8] \cdot 2H_2O$ )	1.804	1.424	-0.582	-0.595	-0.577	-0.573	-0.582
<b>Cd-W</b> ( $Cd_2(H_2O)_4[W(CN)_8] \cdot 2H_2O$ )	1.822	1.420	-0.583	-0.597	-0.577	-0.574	-0.585

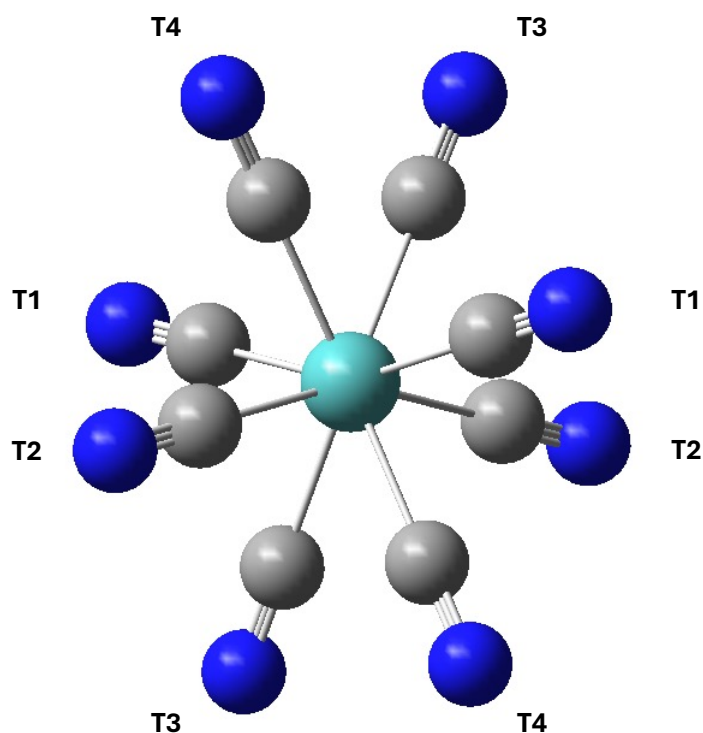


Figure S 1: Octacordinated M block (M=Mo or W) with  $D_{2d}$  symmetry. Cyano ligands are labeled according to their Bader charges (see Table 1).

## 2 Raman spectroscopy

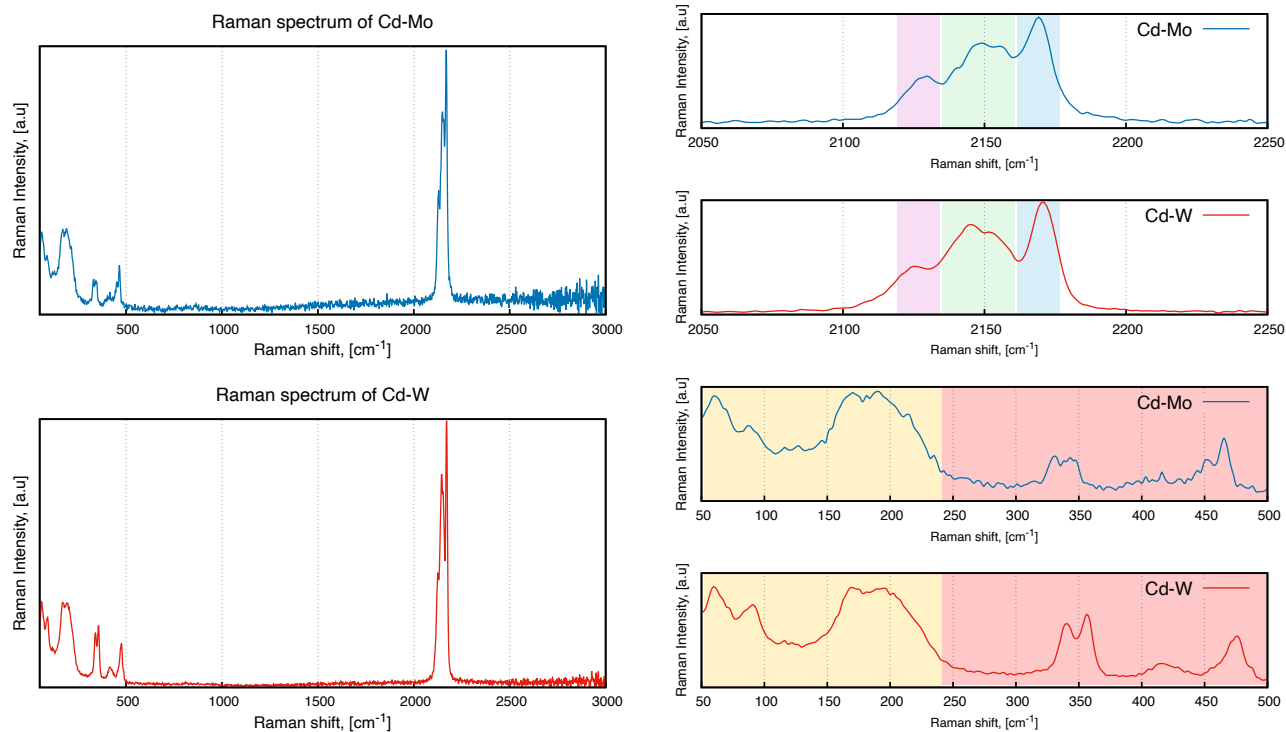


Figure S 2: Raman spectra of Cd-Mo and Cd-W (right column). The ranges 2050 - 2250  $\text{cm}^{-1}$  [ $\nu(\text{CN})$ ] and 50 - 500  $\text{cm}^{-1}$  [ $\delta(\text{C} - \text{M} - \text{C})$  and  $\delta(\text{N} - \text{Cd} - \text{N})$ ] are shown on the left side of the image. Raman shift values are summarized in Table S2

Table S 2: Raman signals. The showed values correspond to the spectra depicted in Figure S2 in the 2050 - 2250  $\text{cm}^{-1}$  and 50 - 500  $\text{cm}^{-1}$  spectral ranges.

Raman shift values, [ $\text{cm}^{-1}$ ]		
Active Raman Modes	Cd-Mo	Cd-W
$\nu(\text{CN})$	2160, 2156, 2149, 2141, 2130, 2125	2170, 2159, 2152, 2145, 2134, 2121
$\nu(\text{M/Cd-}), \delta(-\text{M/Cd-})$	466, 417, 349, 332, 191, 169, 88, 61	476, 416, 358, 340, 197, 169, 92, 61

### 3 Ultraviolet-visible analysis

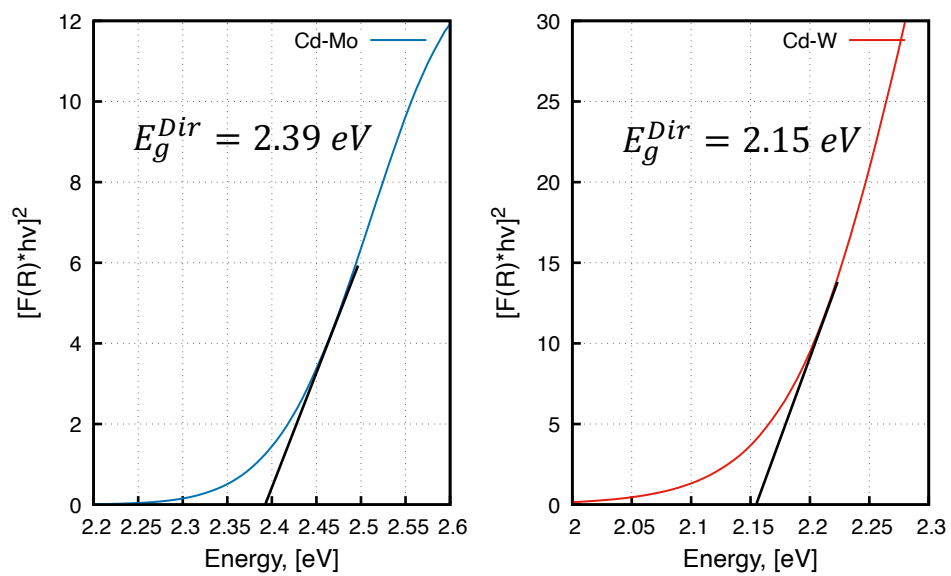


Figure S 3: Tauc plot of Cd-Mo (right blue) and Cd-W (left-red) for allowed direct electronic transitions.

## 4 Projected density of states (HSE06)

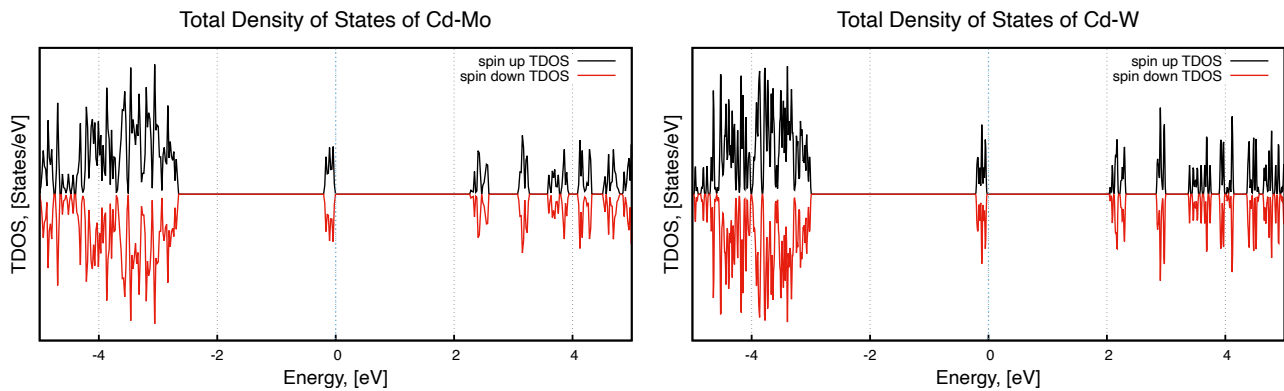


Figure S 4: Total density of states (TDOS) of Cd-Mo (left) and Cd-W (right). Spin up (black line) and spin down (red line) are symmetrical with respect 0 states/eV.

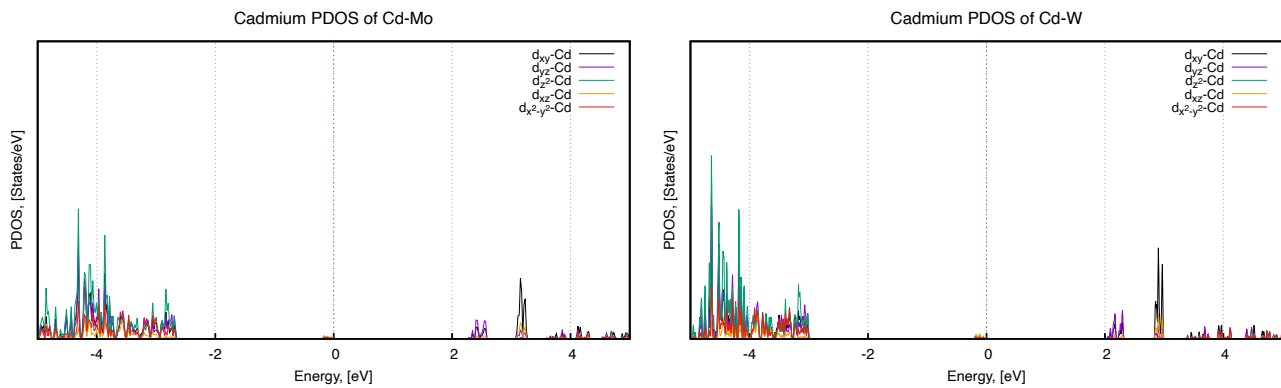


Figure S 5: Projected density of states of cadmium atoms. No relevant orbital contributions are observed at the valence and conduction regions.

## 5 Powder X-Ray Diffraction Patterns (PXRD)

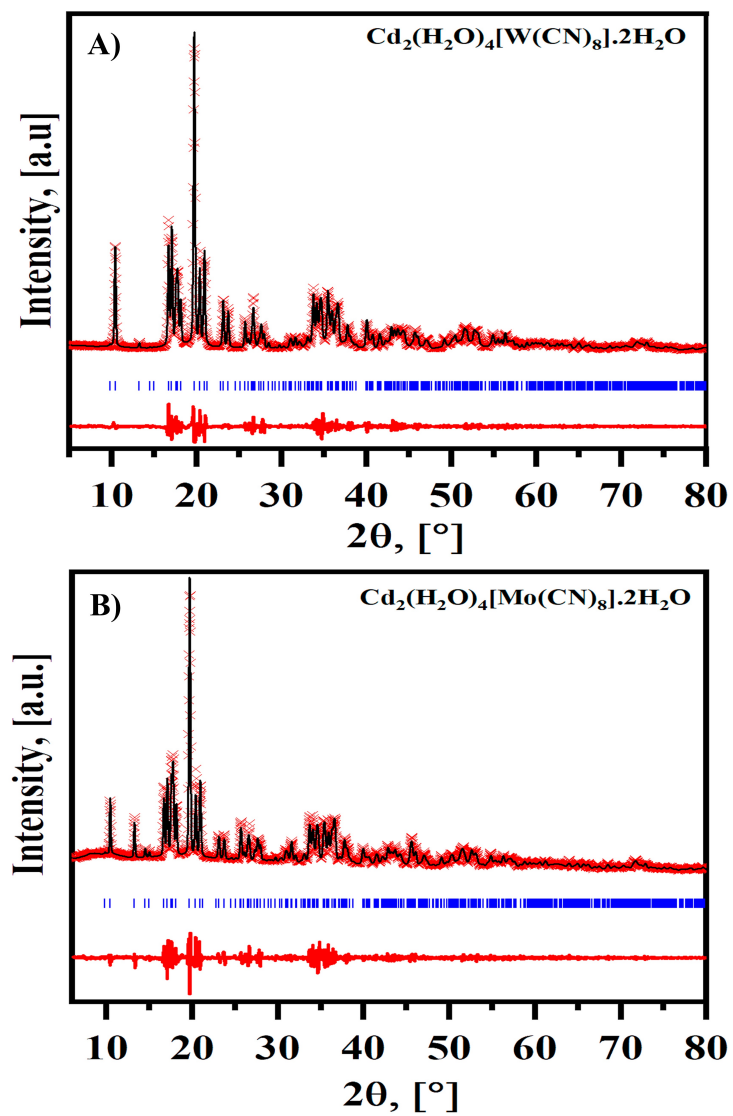


Figure S 6: Powder X-ray diffraction patterns.

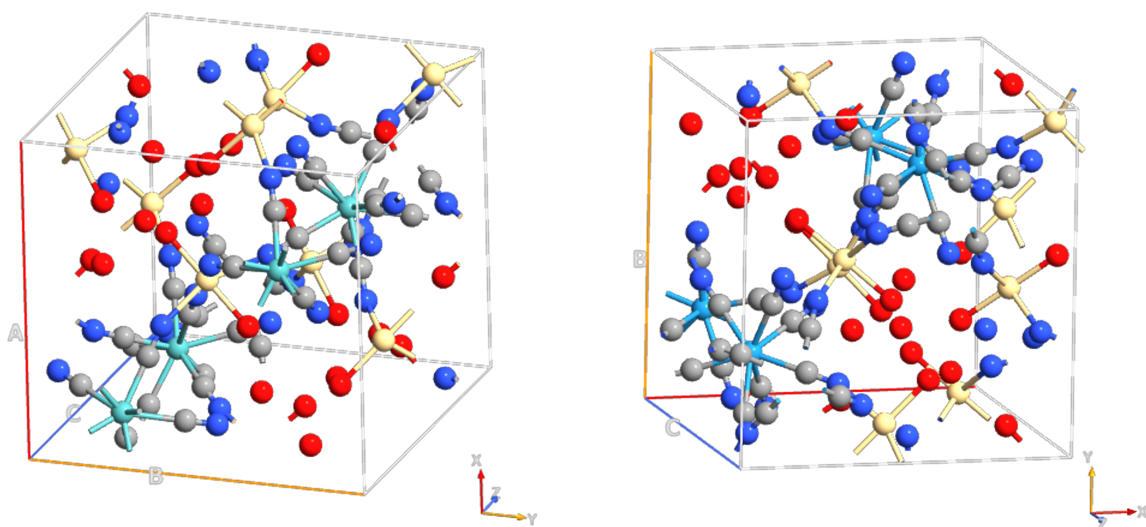


Figure S 7: Unit cell structure of Cd-Mo (left) and Cd-W (right).